

The cluster galaxy luminosity function at $z = 0.3$: a recent origin for the faint-end upturn ?

D. Harsono¹ and R. De Propris^{2*}

¹ *Department of Physics and Astronomy, University of California at Los Angeles, USA*

² *Cerro Tololo Inter-American Observatory, Casilla 603, La Serena, Chile*

ABSTRACT

We derive deep luminosity functions (to $M_z = -15$) for galaxies in Abell 1835 ($z = 0.25$) and AC 114 ($z = 0.31$) and compare these with the local z' luminosity function for 69 clusters. The data show that the faint-end upturn, the excess of galaxies above a single Schechter function at $M_z < -17$, does *not* exist in the higher redshift clusters. This suggests that the faint-end upturn galaxies have been created recently, by infall into clusters of star-forming field populations or via tidal disruption of brighter objects.

Key words: galaxies: luminosity function, mass function – galaxies: dwarf

1 INTRODUCTION

The mass function of Cold Dark Matter (CDM) halos emerging from the epoch of recombination is expected to be very steep, with a slope $\alpha \sim -2$ (Klypin et al. 1999; Moore et al. 1999). However, the slope of the luminosity function (LF) of galaxies in the Local Group is very flat, $\alpha \sim -1.1$ to $M_V = -10$ (Pritchet & van den Bergh 1999), while Trentham, Sampson & Banerij (2005) also find a very flat slope (to $M_g = -9$) in poor groups selected from the Sloan survey. This is the well known small scale problem in CDM, for which a number of solutions (involving suppression of dwarf galaxy formation in small haloes) have been proposed. On the other hand, there is evidence that the LF of dwarf galaxies ($M_V < -17$) in rich clusters shows a steep upturn, approaching the predicted CDM value. Originally discovered by Driver et al. (1994) and, independently, by De Propris et al. (1995), the existence of this faint-end upturn has recently been placed on a firmer footing by Popesso et al. (2006, hereafter P06), who detect it in all four bands of the composite LF of 69 X-ray selected clusters with Sloan photometry. It is very unlikely that fluctuations in the background counts would be able to affect all 69 objects equally and produce an artificial steepening of the LF at faint luminosities.

The origin of the upturn should have interesting consequences for theories of structure formation. If the upturn galaxies are primordial, they may be the relic building blocks of the original population of dwarf-sized fragments that went into constructing the cluster giants. However, the fact that

the upturn is observed in rich environments but not in poor groups suggests that its origin is related to the cluster environment. Unless the cluster acts to preserve a primordial population of faint dwarfs (Babul & Rees 1992), it appears more likely that the upturn galaxies have undergone recent infall from the surrounding field (Wilson et al. 1997). They may also have been whittled down from more massive objects (Conselice, Wyse & Gallagher 2001; Conselice et al. 2003). Although the colors of present-day upturn galaxies are consistent with those of dwarf spheroidals on the red sequence (P06, Yamanoi et al. 2007), Conselice et al. (2001) argues that one half of the fainter Virgo dwarfs are actually blue.

The approach we follow here is to study the evolution of the faint-end upturn. In practice, we derive deep LFs for distant clusters and attempt to compare the differential luminosity evolution of the bright cluster members (which evolve passively) and the upturn galaxies. If the upturn galaxies are primordial, they should evolve with the same speed as the giants, most of whose stellar populations were formed at high redshift. Conversely, if the upturn consists of fading irregular galaxies (Wilson et al. 1997), we should see a brighter onset of the steepening at higher redshifts, or, if the upturn galaxies have undergone recent infall from the field, a much flatter faint-end slope.

We begin by considering two clusters at $z = 0.3$ with deep archival Hubble Space Telescope (HST) Advanced Camera for Surveys (ACS) imaging. While this choice is set by the availability of archival data, this is an interesting redshift as it corresponds to the epoch at which we witness the onset of the faint blue galaxies excess and the increase in the blue fraction in clusters of galaxies, both of which may be attributed to a population of star forming low luminosity

* E-mail: rdepropris@ctio.noao.edu

galaxies temporarily brightened by star formation episodes (e.g., Babul & Ferguson 1996; Driver et al. 1996)

We derive a deep z band LF for galaxies in the above clusters and compare with the P06 local sample. This latter represents the averaged LF of $z < 0.1$ clusters to a depth comparable to our own and determined using similar methods (statistical subtraction of non cluster members using counts in reference fields). An additional benefit is that the ACS filters are designed to imitate the Sloan passbands used in the photometry of local clusters by P06. For these reasons, we adopt their z' band LF as our comparison to measure evolution.

The following section describes the data, their reduction, analysis and photometry. Discussion of the results and their interpretation can be found in section 3. We adopt the latest cosmology with $\Omega_M = 0.3$, $\Omega_\Lambda = 0.7$ and $H_0 = 70 \text{ km s}^{-1} \text{ Mpc}^{-1}$.

2 OBSERVATIONS AND DATA ANALYSIS

We use two deep (10,000s total integration) archival observations of the clusters Abell 1835 (at $z = 0.253$) and AC 114 ($z = 0.312$) carried out with the ACS in the z (F850LP) filter (PI: Pelló; PID: 10154). Abell 1835 is a richness 0 cluster, similar to the Fornax or Virgo clusters (but somewhat more massive), while AC 114 has richness class 2 and is therefore similar to the Coma cluster. Both clusters are therefore comparable to the P06, although they lie on the high mass end of the distribution.

We retrieved the individual flatfielded exposures from the HST archive and processed them through `Multidrizzle` (Koekemoer et al. 2002) to produce a single registered image for each cluster, interpolated across the chip gaps and with cosmic rays and cosmetic defects removed. The final data products are shown in Fig. 1. The images cover a total of 900 kpc on the side. For AC 114 the image is centred on the brightest cluster galaxies and spans a radius of 400 kpc, which is equivalent to 1/2 of the median r_{200} (the radius at which the cluster is 200 times denser than the field) over which P06 compute their LFs. The geometry of A1835 is more complex. Because of a bright star, the central cluster galaxy is shifted towards the eastern side of the image. The ACS image of this cluster reaches out to the median r_{200} value.

As with all similar studies, and especially at the faint end, we can only determine cluster membership statistically. Counts of field galaxies projected onto the cluster field of view can be estimated by observation of blank (cluster-less) fields. We note here that the luminosity distance to A1835 and AC114 is much larger than the largest structure present in local redshift surveys and therefore the counts in the direction of the clusters should reflect the cosmic mean (the structure is uncorrelated with the cluster). We use the two GOODS fields (Giavalisco et al. 2004) as our reference fields, as these are the deepest and widest available images in the z band.

Detection and photometry were carried out using `SExtractor` (Bertin & Arnouts 1996) using exactly the same parameters for the clusters and GOODS fields: a minimum detection ‘aperture’ of 7 connected pixels above 1.5σ from the sky, which is equivalent to a 3σ detection. We measured

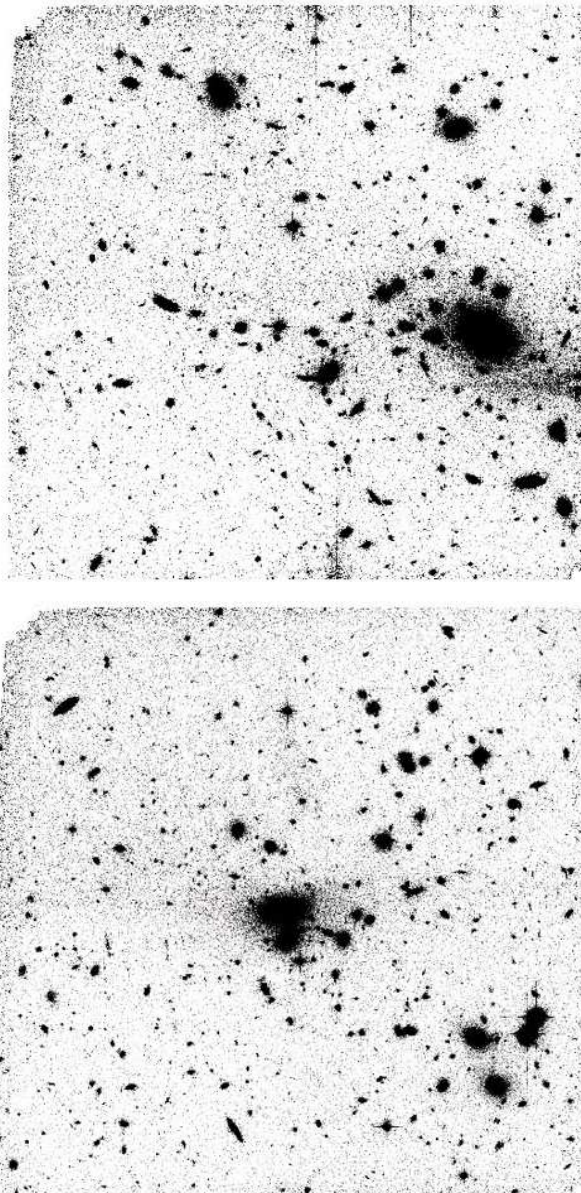


Figure 1. Grayscale images of A1835 (top) and AC114 (bottom)

photometry in an adaptive aperture and in a circular aperture of area equivalent to the minimum number of connected pixels, to derive a mean central surface brightness. The data were calibrated on the HST AB system using published zero-points.

Fig. 2 shows plots of μ_z vs z for objects in the cluster fields and the GOODS fields. The sequence of objects which constitutes an upper envelope to the detections can be identified with stars. We can easily separate stars and galaxies to at least $z = 25.5$, which is fainter than the completeness limit we estimate below. We inspected our detections to remove a few objects (in both cluster and GOODS fields) that were deblended excessively by the `SExtractor` algorithm (usually bright spiral galaxies). For the few objects where this was necessary, we computed magnitudes in a single large aperture.

It is obvious that the GOODS fields reach deeper ap-

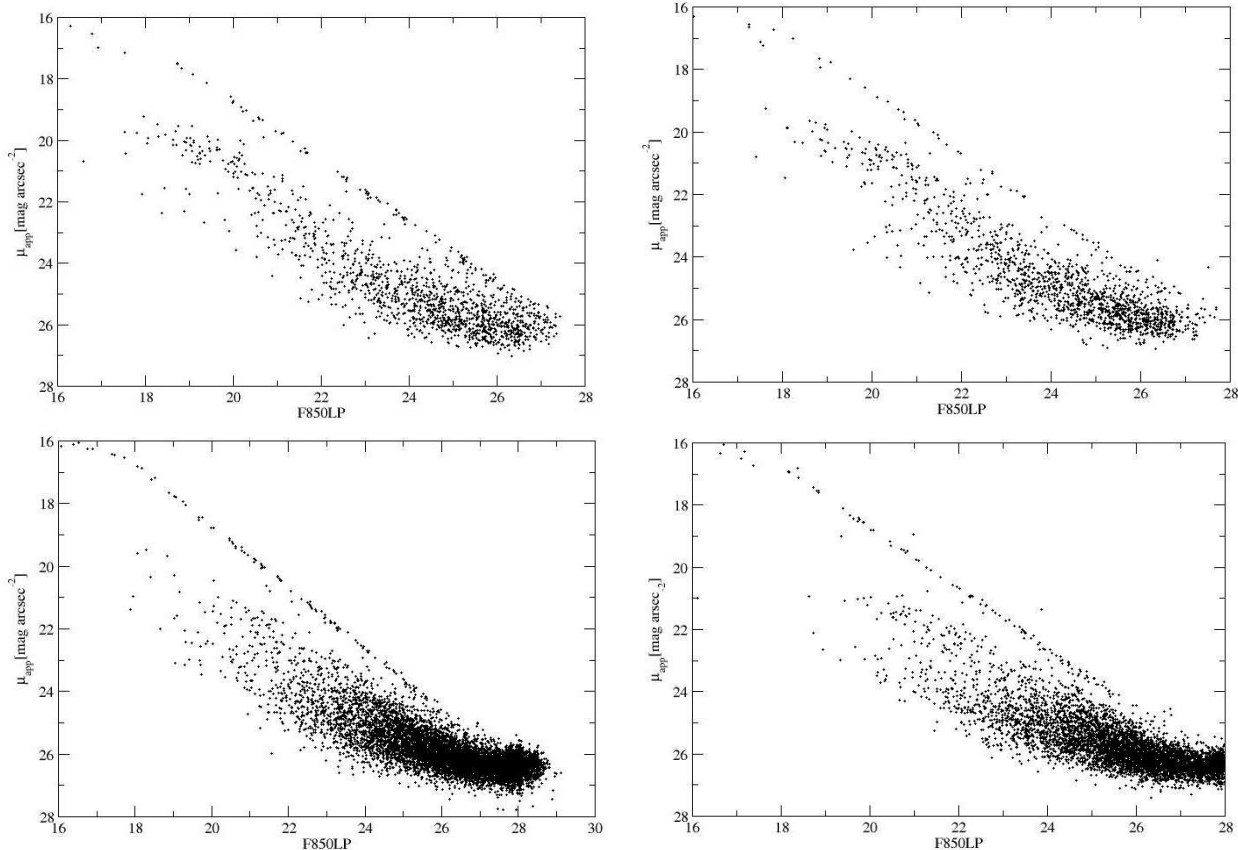


Figure 2. Central surface brightness vs. z for objects in the A1835 (top left), AC114 (top right), GOODS-N (bottom left) and GOODS-S (bottom right) fields

parent luminosities and somewhat deeper surface brightness limits than our cluster field (as they have about 10 times the exposure time). We need to choose a common limiting central surface brightness for both the cluster and the background fields. We only count galaxies with central μ_z above this value. It is seen from Fig. 2 that $\mu_z \sim 26.2$ mag arcsec $^{-2}$ selects most objects in the cluster fields. We note that we start missing lower surface brightness objects at $z > 24$ so that we are incomplete at fainter apparent luminosities. However, we are equally incomplete in the GOODS fields so this should not affect our determination of the LF, although, strictly, we can only state a lower limit to the LF slope.

Fig. 3 shows galaxy number counts (with central $\mu_z < 26.2$) for the cluster and GOODS fields. From this figure, we see that our data are complete at least to $z = 24.5$ and possibly beyond (the counts are still rising). We adopt this as our magnitude completeness limit.

In order to remove contamination of our cluster fields by foreground and background galaxies we use galaxy counts in the GOODS fields. We fit these counts with a second degree polynomial to smooth variations due to large scale structure. At faint luminosities, the typical scale sampled by each GOODS field is also larger than the largest existing structure, and the counts should therefore reflect the cosmic mean. This can be seen most clearly in Figure 12 of Capak et al. (2007) where the I band counts for COSMOS fields, Hubble Deep Field (from Capak et al. 2004) and the

HST counts in the Hubble Deep Fields North and South are well within each other's error bars. Fig. 3 also shows how the GOODS North and South counts are consistent with each other. We note also that the effect of cosmic variance on the background counts can be estimated in the error budget, using the 'counts-in-cells' approach of Peebles (1975).

We subtract the scaled (and smoothed) GOODS counts from the cluster counts and compute error statistics by adding, in quadrature, the Poisson errors in the galaxy counts for the cluster fields, the scaled errors for the predicted background contribution and the Poisson errors for counts in the GOODS fields. To these we add, also in quadrature, the clustering errors (which take care of cosmic variance) for galaxy counts in the GOODS fields and the scaled galaxy counts for the cluster fields, following the methods of Huang et al. (1997); Driver et al. (2003) and Pracy et al. (2004). For reference, the error in the counts for field i at apparent magnitude m is computed as (Huang et al. 1997):

$$\sigma_i^2 = N_i(m) + 5.3(r/r_*)^\gamma \Omega_i^{(1-\gamma)/2} N_i^2(m)$$

where $N_i(m)$ are the galaxy counts for fields i at apparent magnitude m , r_* is defined as $5 \log r_* = m - M^* - 25$ (M^* is as defined in the Schechter function), Ω_i is the area of field i and γ is the index of the correlation function (1.77).

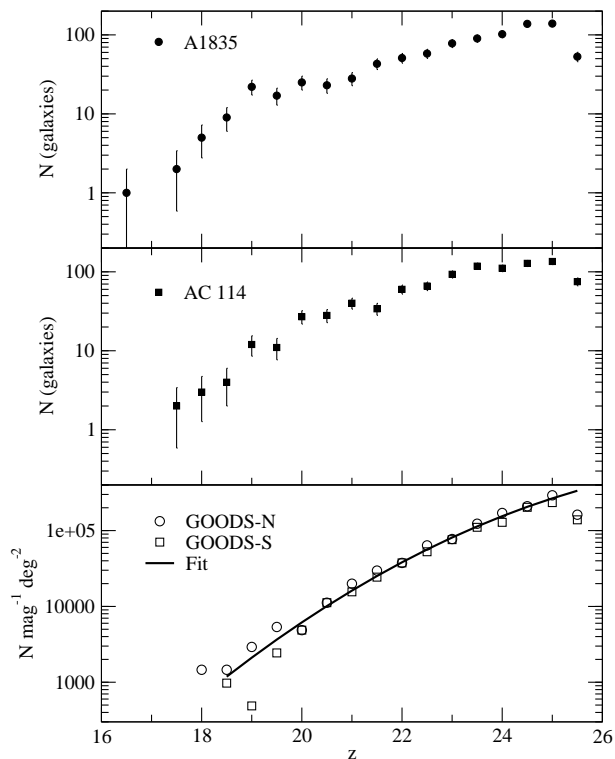


Figure 3. Galaxy number counts vs. z for A1835, AC114, GOODS-N and GOODS-S and the best fitting quadratic to the logarithmic number counts $\log_{10} N = -14.256 + 1.3623 * z - 0.023002 * z^2$. The error bars for counts in the GOODS fields are comparable to the size of the points and are omitted for clarity.

3 DISCUSSION

We plot the LFs and best fits (to a single Schechter function) to the galaxy counts in A1835 and AC114 in Fig. 4. We see that a single Schechter function provides a reasonable fit to the data. The best fit parameters (with marginalised 1σ errors) are: $M_z^* = 17.85 \pm 0.97$ and $\alpha = -1.38 \pm 0.13$ for A1835 and $M_z^* = 18.99 \pm 0.86$ and $\alpha = -1.30 \pm 0.12$ for AC114. The characteristic luminosity is poorly determined, because of small number statistics, but is consistent with the local value of P06 after $k+e$ correction (using a Bruzual & Charlot 2003 model with solar metallicity, Salpeter initial mass function, formation redshift of 3 and e-folding time of 1 Gyr, which provides a good fit to the colours of present-day ellipticals) and correcting for the +0.52 mag. offset between HST z and SDSS z' (Holberg & Bergeron 2006). The slope we derive is somewhat steeper than the local one but is consistent with the slope of the LF in A2218 measured by Pracy et al. (2004): rich clusters are known to contain more dwarfs and have steeper faint-end slopes (Phillipps et al. 1998).

Our main interest is to compare the local LFs with our observations in order to study the evolution of the faint-end upturn. To this end we plot the LFs by P06 over our data, after correcting for the distance modulus, $k+e$ correction and magnitude offset. The normalization is chosen to match our counts at $M_z = -21$ in order to better compare the faint-end behaviour. It is obvious that there is *no* evidence of a faint-end upturn at $M_z < -17$ in the $z = 0.3$ clusters. It may be argued that the upturn is most evident in

the outskirts of clusters, rather than in their cores (P06). Pracy et al. (2004) find that the LF of what they term ‘ultra-dwarfs’ is flatter in the core than in the outskirts. However, we sample between $1/2$ of r_{200} and r_{200} and P06 detect a faint-end upturn, at least for red galaxies to which we are most sensitive in the z band, even for $r < 0.3r_{200}$ (their Figure 11). Furthermore, the upturn is clearly detected by numerous authors even in the core (indeed, especially in) of the Coma cluster (De Propris et al. 1998; Trentham 1998; Milne et al. 2007).

The two clusters we survey are also similar to local clusters: they have the same richness as Coma or Fornax and have X-ray properties similar to the sample of P06. It is unlikely that differences in the cluster samples are responsible for our findings.

Neither does it appear likely that we are missing galaxies (with respect to the SDSS) because of low surface brightness effects: SDSS data are 50% complete at $\mu_r = 23.5$ (Blanton et al. 2005) while we go considerably deeper (at least $\mu_z = 26.2$). In AC114 and AC118 Andreon, Punzi & Grado (2005) present a K -band LF of depth comparable to ours. The parameters for the LF in AC114 are virtually identical to ours and both LFs can be fitted by a single Schechter function with no upturn.

The most obvious interpretation is that the faint-end upturn is of recent origin. One possibility is that it consists of fading objects that have recently infallen from the field, where the LF for star-forming galaxies is actually quite steep (Hogg & Phinney 1997). These galaxies may also be whittled down from formerly more massive objects, in the manner proposed by Conselice et al. (2001). It is interesting to speculate that these faint dwarfs are but the latest instalment in the buildup of the cluster red sequence. As we look back in time we see that the cluster dwarf population is progressively missing as low mass field galaxies are converted into dwarf ellipticals (e.g., De Lucia et al. 2007): these very faint dwarfs may correspond to the very low amplitude fluctuations which are nowadays falling into the large scale structures for the first time.

Ultimately, we should be able to achieve a more complete understanding of these objects by studying a large number of clusters in several bandpasses and over wide fields. Some HST archival data for this project are available and are being analyzed for a future publication but these include only the central regions of several intermediate redshift clusters. Wide-field imaging on large telescopes may be needed to make further progress

ACKNOWLEDGEMENTS

DH carried out this work while on the Research Experience for Undergraduate program at Cerro Tololo Inter-American Observatory and wishes to acknowledge the hospitality of CTIO during the Chilean summer. The REU program is supported by NSF grant 0353843. We would like to thank the CTIO REU program director, Stella Kafka, for her efforts on behalf of the students.

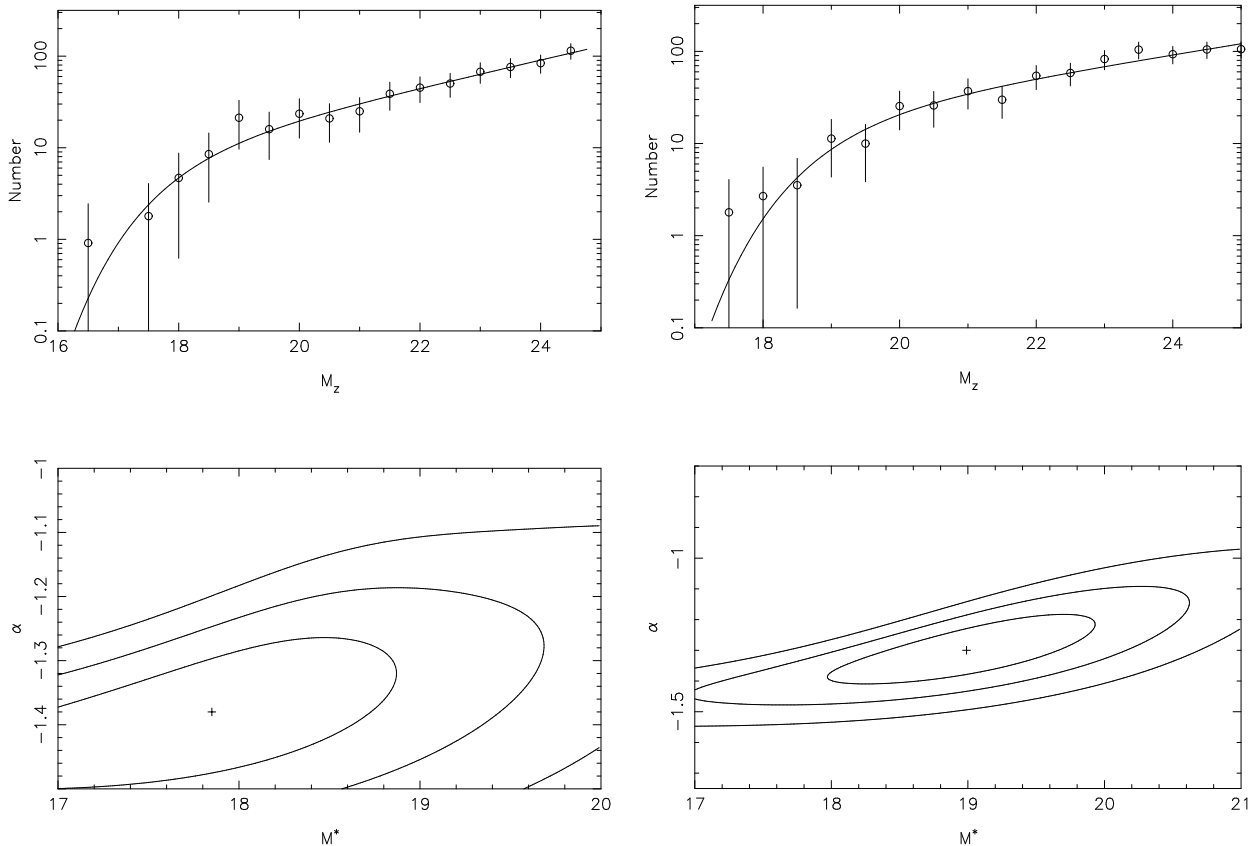


Figure 4. Luminosity functions and best fits, with error ellipses, for A1835 (left) and AC114 (right)

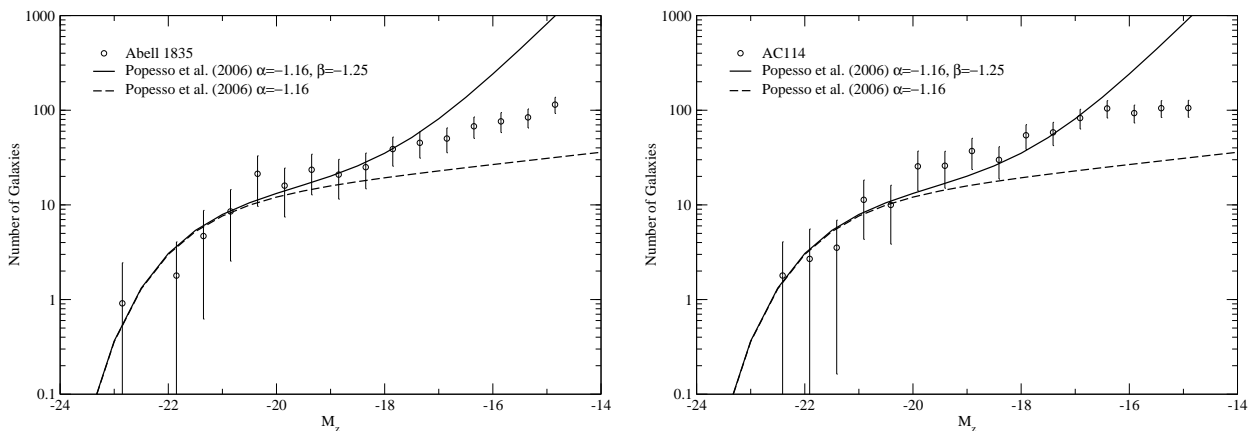


Figure 5. Comparison of local LFs to the A1835 (top) and AC114 (bottom) LFs. We also show an upturn-less LF for comparison.

REFERENCES

- Andreon S., Punzi G., Grado A. 2005, MNRAS, 360, 727
 Babul A., Rees M. J. 1992, MNRAS, 255, 346
 Babul A., Ferguson H. C. 1996, ApJ, 458, 100
 Bertin E., Arnouts S. 1996, A&AS, 117, 393
 Blanton M. L., Lupton R. H., Schlegel D. J., Strauss M. A., Brinkmann J., Fukugita M., Loveday J. 2005 ApJ, 631, 208
 Bruzual G., Charlot S. 2003, MNRAS, 344, 1000
 Capak P. et al. 2004, AJ, 127, 180
 Capak P. et al. 2007, ApJS, in press (astro-ph 0704.2430)
 Conselice C. J., Gallagher J. S., Wyse R. F. G. 2001, AJ, 122, 2281
 Conselice C. J., O'Neil K., Gallagher J. S., Wyse R. F. G. 2003, ApJ, 591, 167
 De Lucia G. et al. 2007, MNRAS, 374, 809
 De Propris R., Pritchett C. J., Harris W. E., McClure R. D.

- 1995, ApJ, 450, 534
De Propris R., Eisenhardt P. R., Stanford S. A., Dickinson M. 1998, ApJ, 503, L45
Driver S. P., Phillipps S., Davies J. I., Morgan I., Disney M. J. 1994, MNRAS, 268, 393
Driver S. P., Couch W. J., Phillipps S., Windhorst R. A. 1996, ApJ, 466, L5
Driver S. P., Odewahn S. C., Echevarria L., Cohen S. H., Windhorst R. A., Phillipps S., Couch W. J. 2003, AJ, 126, 2662
Giavalisco M. et al. 2004, ApJ, 600, L93
Hogg D. W., Phinney E. S. 1997, ApJ, 488, L95
Holberg J. B., Bergeron P. 2006, AJ, 132, 1221
Huang J.-S., Cowie L. L., Gardner J. P., Hu E. M., Songaila A., Wainscoat R. J. 1997, ApJ, 476, 12
Koekemoer A., Fruchter A. S., Hook R. N., Hack W. 2002, in *The 2002 HST Calibration Workshop* ed S. Arribas, A. N. Koekemoer, B. C. Whitmore (Baltimore: Space Telescope Science Institute), p. 337
Klypin A., Kravtsov A., Valenzuela O., Prada F. 1999, ApJ, 522, 82
Milne M. L., Pritchett C. J., Poole G. B., Gwyn S. D. J., Kavelaars J. J., Harris W. E., Hanes D. A. 2007, AJ, 133, 177
Moore B. et al. 1999, ApJ, 524, L19
Peebles P. J. E. 1975, ApJ, 196, 647
Phillipps S., Driver S. P., Couch W. J., Smith R. M. 1998, ApJ, 498, L119
Popesso P., Biviano A., Böhringer H., Romaniello M. 2006, A&A, 445, 29
Pracy M. B., De Propris R., Driver S. P., Couch W. J., Nulsen P. E. J. 2004, MNRAS, 352, 1135
Pritchett C. J., van den Bergh S. 1999, AJ, 118, 883
Trentham N. 1998, MNRAS, 293, 71
Trentham N., Sampson L., Banerji M. 2005, MNRAS, 357, 783
Wilson G., Smail I., Ellis R. S., Couch W. J. 1997, MNRAS, 284, 915
Yamanoi H. et al. 2007, AJ, submitted (astro-ph 0701670)